

## ASSESSMENT OF FUTURE RAINFALL PATTERNS IN CAMERON HIGHLANDS USING THE STATISTICALLY DOWNSCALED LOCAL CLIMATE MODEL

Kok Weng TAN<sup>1\*</sup>, Niqiao LIU<sup>1</sup>, Yuk Feng HUANG<sup>2</sup>, Yuanyi LI<sup>3</sup>

<sup>1</sup>Faculty of Engineering and Green Technology, Universiti Tunku Abdul Rahman, 31900 Kampar Perak, Malaysia

<sup>2</sup>Lee Kong Chian Faculty of Engineering & Science, Universiti Tunku Abdul Rahman, 31900 Kampar Perak, Malaysia

<sup>3</sup>School of Marine Science and Technology, Tianjin University, 300072 Tianjin, People Republic of China

### Abstract

Past decades, the natural disasters such as flash flood and landslides in the Cameron Highlands have caused significant damage to public infrastructure and posed serious risks to human health. This study aims to investigate projected changes in precipitation under various future scenarios and spatiotemporal scales. Specifically, it focuses on statistically downscaling the CANESM5 model and analysing rainfall pattern changes for the period 2015–2100 under the SSP2-4.5 and SSP5-8.5 scenarios through spatial analysis. By comparing historical observed and simulated data, the study confirms that the model effectively represents rainfall pattern across the projection period. Results from the localized climate model (2015–2100) indicate that precipitation trends at Stations 1 (p1-Kg. Raja township) and 2 (p2-Bertam valley) are similar under both scenarios until 2063, after which they diverge. In contrast, Station 3 (p3-Brinchang township) shows markedly higher precipitation changes. Notably, under SSP5-8.5 scenario, the rainfall anomalies shift from negative to positive around 2049, with this scenario having a stronger influence on precipitation patterns than SSP2-4.5 and being less impacted by terrain effects. Spatial analysis further reveals a correlation between elevation and precipitation, indicating that higher altitudes are associated with increased rainfall.

**Keywords:** statistical climate modeling, spatial analysis, rainfall patterns, Cameron Highlands

## 1. INTRODUCTION

Anthropogenic activities have been definitively identified as the principal driver of the observed global warming of approximately 1°C (within a range of 0.8–1.2°C) above pre-industrial levels. Projections

---

\* Corresponding author: Kok Weng Tan, Faculty of Engineering and Green Technology, Universiti Tunku Abdul Rahman, 31900 Kampar Perak, Malaysia. Email: [tankokweng@utar.edu.my](mailto:tankokweng@utar.edu.my), Tel: +605-468 8888

further indicate that global temperatures are likely to rise by 1.5°C between 2030 and 2052 [1]. The scientific community has devoted substantial attention to anticipating future climate changes, particularly concerning extreme climatic events due to their profound societal impacts. Among these, intensified precipitation extremes pose direct threats to communities, as they are closely linked to both flooding and drought. Recent catastrophic events underscore this vulnerability, including the 2022 floods in Pakistan, which resulted in at least 1,739 fatalities (June–October), Nigeria with over 612 deaths (June–November), South Africa with a minimum of 461 casualties (April), Brazil with at least 233 deaths (February), India with 192 deaths (June–September), and Afghanistan with more than 182 fatalities (August) [2]. Given these alarming events, accurate projections of future rainfall patterns are critical to inform and implement effective mitigation and adaptation strategies.

Similarly, the Cameron Highlands has experienced multiple serious flood events over the past decade, often triggered by intense rainfall, dam releases, and land clearing. Major flood incidents occurred in 2013 and 2014, the deadly mud floods event occurred in Bertam Valley and Ringlet that killed several people, destroyed homes, and displaced dozens of families. Flash floods and landslides also hit the same area in 2016 and 2024, causing property damage and temporary evacuations. These floods disrupt local communities, damage infrastructure, and threaten the agriculture and tourism sectors that are vital to the highland economy.

Besides, the likelihood of prolonged drought seasons in Cameron Highlands is increasing. These extended dry periods can severely disrupt the local economy, especially in sectors that depend on a steady supply of clean water. Agriculture, a cornerstone of the region's economy, is particularly vulnerable. Under optimal conditions, the area's agricultural sector contributes an estimated USD 56 million annually in production value. With water scarcity stretching over months, entire planting cycles often fail. High-value crops such as tea, strawberries, and vegetables are especially vulnerable, leading to significant income losses for farmers. These shortages have a ripple effect, driving up food prices, disrupting supply chains nationwide, and cutting into the earnings of hotels, local guides, and small businesses that rely on tourist spending.

Most hydrological studies have traditionally relied on ground-based station data for analysis. However, weather especially rainfall prediction remains one of the most complex aspects of the hydrological cycle [3]. Weather gauge stations are widely used for measuring precipitation due to their accessibility. Statistical downscaling of weather data has been widely adopted in Malaysia, as it assumes a robust and quantifiable relationship between global climate models (GCMs) and local climate conditions. Through this relationship, local climate projections can be derived from GCM outputs when integrated with historical regional data [4]. Compared to dynamical downscaling, this method requires significantly lower computational resources, making it a cost-effective option for producing high-resolution local climate assessments without relying on expensive hardware.

Different studies have employed statistical downscaling in Malaysia, including the downscaling of HadCM3 for long-lead rainfall prediction in the Kurau River Catchment [5], development of localized climate models using SRE scenarios for Penang, Selangor, and Johor with the PRECIS model [6], downscaling of rainfall under transitional climates in the Limbang River Basin using CanESM2 [7] and daily average rainfall modeling based on CMIP5 scenarios for Kota Bharu, Kelantan [8]. These studies highlight the application of statistical downscaling across regions such as Perak, Selangor, Penang, Johor, Kelantan, and Kedah, focusing on precipitation and temperature data. GCM datasets like HadCM3, CanESM2, and CMIP have been utilized to simulate local precipitation and temperature through methods such as SDSM, LARS-WG, CORDEX-SEA, and Random Forest. However, statistical downscaling efforts incorporating CMIP6 scenarios remain limited and underexplored.

Nevertheless, in developing countries such as Malaysia, the scarcity of stations in remote areas and the limited number of gauges covering large catchment regions present significant constraints [9].

Global Climate Models (GCMs) represent sophisticated numerical tools that integrate physical processes across the atmosphere, oceans, cryosphere, and terrestrial surfaces. These models are among the most advanced systems available for simulating interactions within the global climate system. When downscaled through nested regional models or coupled with simpler frameworks, GCMs offer geographically and temporally robust projections of climate responses [10].

The objective of this study is to develop a local climate model for the Cameron Highlands using a statistical downscaling approach, enhancing the resolution and applicability of global climate projections to the region. Using the outputs from this localized model, the study analyses the changes in rainfall patterns from 2015 to 2100 through spatial analysis, offering insights into the potential long-term impacts of climate change on local precipitation trends.

## **2. MATERIALS AND METHODS**

### **2.1 Study area**

Cameron Highlands, situated in the state of Pahang, Peninsular Malaysia, exhibits diverse terrain with elevations ranging from 1070 to 2110 meters above sea level. Characterized by its mountainous topography, it stands as the smallest district in Pahang, occupying the Northwestern corner of the state over a total area of 687 km<sup>2</sup> and hosting a population of around 39,000 residents. As shown in Figure 1, it is sharing borders with the states of Kelantan to the north and Perak to the west, Cameron Highlands is comprised of three mukims: Mukim Ulu Telom, Mukim Ringlet, and Mukim Tanah Rata. These mukims collectively encompass nine townships, including Blue Valley, Kg. Raja, Kuala Terla, Tringkap, Kea Farm, Tanah Rata, Brinchang, Ringlet, and Bertam Valley.

The Cameron Highlands is characterized by a Tropical Highland climate, which is cool, humid, and temperate-like throughout the year. Temperatures typically range between 14°C to 24°C, with an annual mean of approximately 19°C, offering a cooler environment compared to Malaysia's lowlands. The region maintains a high humidity level, ranging from 85% to 95% year-round, contributing to frequent mist and fog, especially in the mornings and evenings. Annual rainfall is substantial, averaging between 2,700 mm to 3,000 mm, and is distributed throughout the year, although rainfall intensifies during the monsoon seasons. The wettest periods occur during the Southwest Monsoon (May to October) and the Northeast Monsoon (November to January), while relatively drier months are experienced from February to April. Although the region generally experiences calm wind conditions, occasional strong winds may accompany the monsoon rains. Due to the fertile highland soils and unique of climatic condition, the main socioeconomic is dedicated to vegetable farming, floriculture and thriving ecotourism activities. This unique climate supports a rich agricultural but also presents risks of landslides and flash floods during heavy rainfall events.

### **2.2 Data collection**

The historical daily rainfall was gathered from both the NASA Earthdata portal and the Malaysian Meteorological Department (MMD). This dataset covers the period from 1983 to 2022 and pertains to three specific stations located in the Cameron Highlands of Malaysia (Table 1 and Figure 2). To ensure data integrity, the SDSM 4.2 software's quality control function was employed. Addressing weather data quality is a critical undertaking in developing nations due to the prevalent occurrence of missing data. Failing to rectify these gaps can impede subsequent processes such as predictor screening and calibration. In the context of this study, station one exhibited 12 instances of missing data As emphasized by [12], regions most susceptible to climate variability often coincide with those exhibiting substantial

data deficiencies. To address this issue, the missing daily rainfall values were filled using data from the NASA Earthdata portal (<https://power.larc.nasa.gov/>).

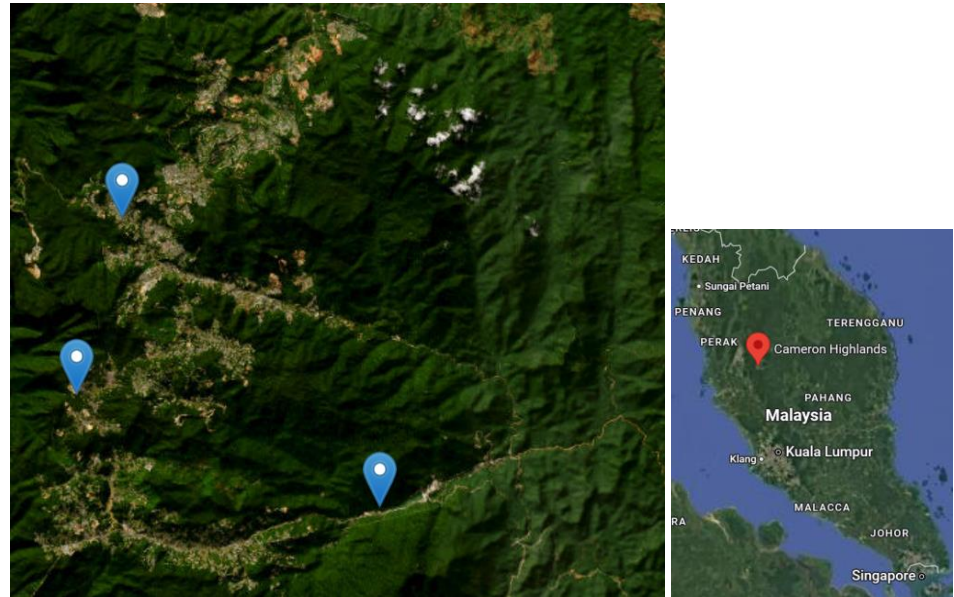


Fig. 1. Location of Cameron Highlands [11]

Table 1. The location of three stations used for downscaling work

Station Data	longitude	latitude
p1-Kg. Raja Township	101.394	4.5714
p2-Bertam Valley Township	101.5229	4.428
p3-Bringchang Township	101.3714	4.4842

## 2.3 Atmospheric predictors screening

This study employed the Canadian Earth System Model version 5 (CanESM5), a state-of-the-art Global Climate Model (GCM). Notably, CanESM5 exhibits a higher equilibrium climate sensitivity of 5.6 K, compared to its predecessor, CanESM2, which recorded a sensitivity of 4.5 K. Within GCM frameworks, predictors refer to large-scale atmospheric variables archived within the model outputs. Ideally, predictors should maintain both conceptual and physical consistency with their corresponding predictands—the observed climatic data. The reliability of GCM simulations is largely contingent upon a robust and stable relationship between predictors and predictands. To facilitate the downscaling of precipitation data, priority was given to a suite of predictors representing circulation, atmospheric stability, thickness, and moisture content, as emphasized by [13], who underscore their critical role in model calibration and validation.

A total of 26 predictors listed in Table 2, were sourced from the National Centres for Environmental Prediction (NCEP) and National Centre for Atmospheric Research (NCAR) reanalysis datasets associated with CanESM5 and were utilized for model calibration. The downscaling framework was unified across all three stations. Accordingly, both CanESM5 and NCEP data served for calibration purposes, while CanESM5 predictors were employed for validation and future projections. Specifically, CanESM5 predictors are available under SSP2-4.5 and SSP5-8.5 scenarios, facilitating future precipitation downscaling from 2015 to 2100 period.

Table 2. The 26 atmospheric predictors used in predictors screening process

Variable ID	Predictor variable
mslp	Mean sea level pressure
p1_f	1000 hPa Wind speed
p1_u	1000 hPa Zonal wind component
p1_v	1000 hPa Meridional wind component
p1_z	1000 hPa Relative vorticity of true wind
p1th	1000 hPa Wind direction
p1zh	1000 hPa Divergence of true wind
p5_f	500 hPa Wind speed
p5_u	500 hPa Zonal wind component
p5_v	500 hPa Meridional wind component
p5_z	500 hPa Relative vorticity of true wind
p5th	500 hPa Wind direction
p5zh	500 hPa Divergence of true wind
p8_f	850 hPa Wind speed
p8_u	850 hPa Zonal wind component
p8_v	850 hPa Meridional wind component
p8_z	850 hPa Relative vorticity of true wind
p8th	850 hPa Wind direction
p8zh	850 hPa Divergence of true wind
p500	500 hPa Geopotential
p850	850 hPa Geopotential
prcp	Total precipitation
s500	500 hPa Specific humidity
s850	850 hPa Specific humidity
shum	1000 hPa Specific humidity
temp	Air temperature at 2m

The Statistical Downscaling Model (SDSM) employs a hybrid methodology that integrates multiple linear regression with a stochastic weather generator. The latter establishes an empirical linkage between data from the National Centres for Environmental Prediction (NCEP) and variables from Global Climate Models (GCMs). By utilizing a combination of multilinear regression models and stochastic bias-correction techniques, SDSM constructs statistical relationships between GCM predictors and local predictands, thereby enabling the downscaling of GCM outputs to finer spatial scales.

Following a comprehensive data quality control process, predictors were selected for each predictand based on statistical criteria, including correlation coefficients, partial correlations, and p-value matrices. This selection process was carried out using Statistical Package for the Social Sciences (SPSS) software. For a single predictand, more than 78 iterations (3 stations  $\times$  26 predictors) were analyzed and synthesised for the rainfall local climate model employed in this study.

To enhance model performance, SDSM was implemented at a monthly temporal scale. The calibration process required two datasets: daily observed data and NCEP daily predictors. Predictor selection for each predictand was conducted through a rigorous screening process. Specifically, the system was calibrated under conditional processes and all applied on a monthly scale to capture seasonality and variability. Once calibrated with the most strongly correlated predictors, the model produced up to 100 ensembles of daily time-series data, with the ensemble mean representing the final output. However, for this study, 20 ensembles were generated for the current period to evaluate model performance. The ensemble mean was employed to assess SDSM's ability to simulate local climatic data, following the approaches outlined by [14] and [15].

## 2.4 Spatial analysis

To complete the spatial analysis, the QGIS (*Quantum Geographic Information System*) software was used to draw rainfall pattern for Cameron Highlands. The delimited text layer was incorporated to import the relevant data files. As tabulated in Table 1, the points  $p1$ ,  $p2$ , and  $p3$  represent the three designated research locations, each identified by their respective longitude and latitude coordinates, ensuring accurate placement on the polygon layer map. Moreover, the time-span groups were set as 2015–2035, 2036–2055, 2056–2075, and 2076–2100, along with their corresponding datasets, reflect the aggregated annual rainfall. Each of time-span group representing 20-years period.

The Inverse Distance Weighting (IDW) interpolation function was utilized to analyse rainfall data for each of these four timeframes within the polygon boundary, using fixed pixel dimensions of 0.0001 for both x and y coordinates. This process generated a total of eight distinct maps. Subsequently, the "Clip Raster by Mask Layer" tool was applied to eliminate extraneous areas beyond the defined boundaries of Cameron Highlands. Finally, further refinements were made to the properties of the eight clipped maps. The rendering type was set to *Singleband Pseudocolor*, and the precipitation value ranges were standardized across all maps to ensure comparability. The interpolation mode was adjusted to *Discrete*, with the quantile method set and the number of quantile classes fixed at seven. Notably, ensuring consistency in the quantile value ranges and colour ramps across all maps was essential for the clear visualization and interpretation of spatial rainfall variability.

## 3. RESULTS AND DISCUSSION

### 3.1. Local climate model – rainfall

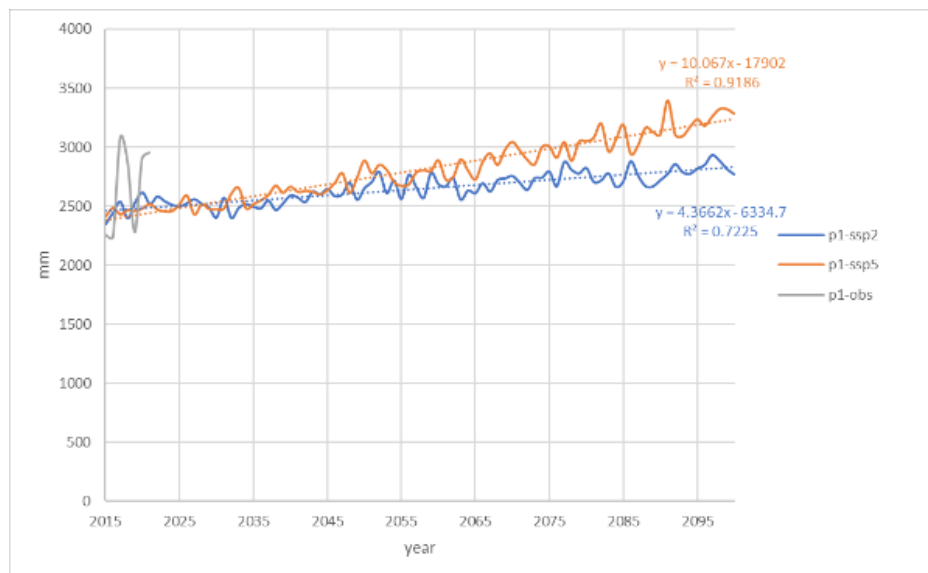
For the  $p1$ - station as shown in Figure 2(a), the historical rainfall data for the period from 2015 to 2021 exhibits significant fluctuations, starting at 2255.47 mm in 2015, reaching its first peak of 3080.32 mm in 2017, dropping to its second lowest point of 2280.12mm in 2019, and subsequently experiencing a rapid ascent to second zenith of 2956.34mm in 2021. Notably, the maximum observed rainfall of 3080.32 mm surpasses the projected annual rainfall values from 2015 to 2100 under the SSP2-4.5 scenario. Similar trend observed from the graph that it surpasses the projected annual rainfall values from 2015 to 2080 under the SSP5-8.5 scenario which is 1.05 times greater than the highest projected precipitation of 2930.55 mm in the year 2097 under the SSP2-4.5 scenario.

It is important to highlight that both the SSP scenarios exhibit a positive linear trendline with equations  $y = 4.3662x - 6334.7$  and  $y = 10.067x - 17902$ , respectively. The coefficient of determination,  $R^2$  values increase from 0.7225 to 0.9186. In statistical terms,  $R^2$  signifies the proportion of the total deviation that can be explained by the regression sum of squares, when performing linear regression analysis using the least squares method for parameter estimation. A higher  $R^2$  indicates a more accurate and significant regression effect, with values closer to 1 implying a better fit. Generally, a model with a

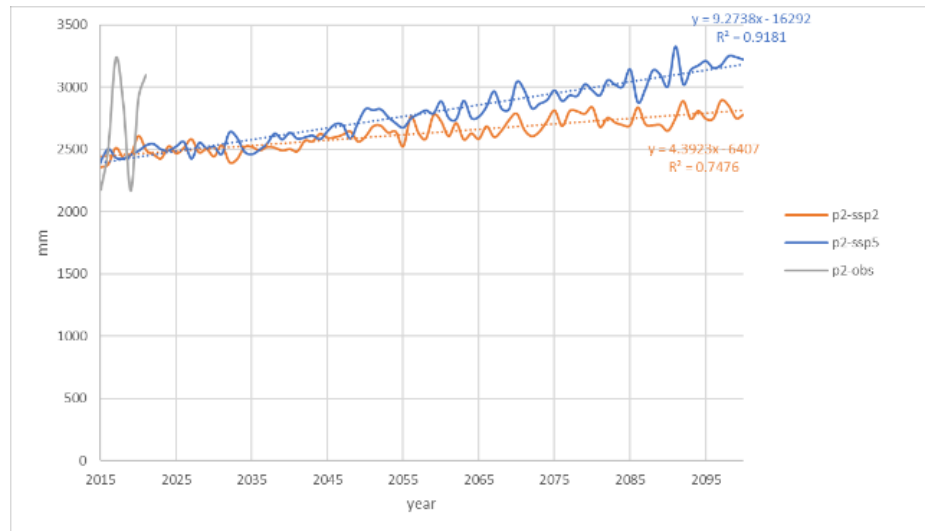
goodness of fit exceeding 0.8 is high; hence, this prospective model offers greater accuracy when analysing precipitation patterns under the SSP5-8.5 scenario.

For the p2 station as shown in Figure 2(b), the projected future rainfall under the SSP2-4.5 and SSP5-8.5 scenarios demonstrates a stable increase with slight fluctuations from 2015 to 2100. This stands in contrast to the historically observed rainfall, which exhibited a range of fluctuations from a minimum of 2235.37 mm in 2016 to a maximum of 3080.32 mm in 2017. Over an extremely short one-year period, the precipitation variation amounted to 844.95 mm. However, the anticipated annual precipitation, as projected, does not undergo such extreme changes within a single year. The noteworthy observation is that both the SSP scenarios exhibit a positive linear trendline represented by the equations  $y = 4.3923x - 6407$  and  $y = 9.2738x - 16292$ , respectively. Furthermore, the coefficients of determination ( $R^2$ ) show an increase from 0.7476 to 0.9181. A higher  $R^2$  indicates a more accurate model and a more pronounced regression effect. Consequently, this model demonstrates increased accuracy when analysing precipitation patterns under the SSP5-8.5 scenario.

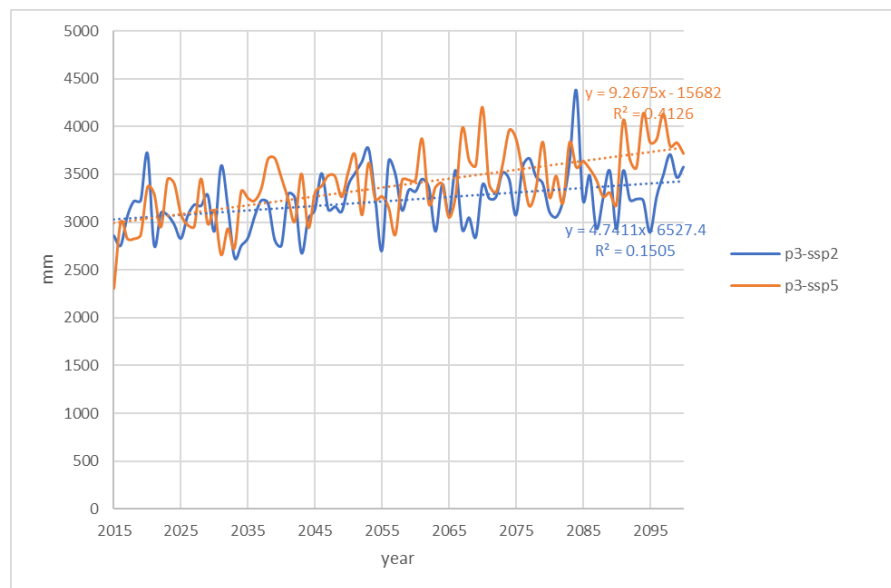
The Figure 2(c) illustrates variations in rainfall from 2015 to 2100 under the SSP2-4.5 scenario. With an  $R^2$  value of 0.1505, it is noteworthy that the minimum recorded rainfall of 2626.77 mm is approximately 1.7 times lower. The SSP58.5 scenario curve representing rainfall changes from 2015 to 2100 under the SSP5-8.5 scenario, demonstrates greater stability with an  $R^2$  value of 0.4126. The maximum recorded rainfall in 1986 was 4199.65mm, which is about 1.8 times the minimum recorded rainfall of 2302.32 mm.



(a)



(b)



(c)

Fig. 2. Projected annual rainfall (2015-2100 period) based on SSP2-4.5 and SSP5-8.5 scenario for the three stations, (a) p1-Kg Raja Township (b) p2- Bertam Valley Township (c) p3- Bringchang Township

The rainfall patterns observed at stations p1 and p2 demonstrate notable uniformity and stability, with no recorded instances of extreme events. A plausible explanation for this could be the limited spatial resolution of the dataset. The absence of extreme rainfall records, particularly in regions with complex topography and intricate rainfall distributions such as the Cameron Highlands. It suggests that enhancing spatial resolution may enable more accurate simulation of localized extreme events.

Additionally, the lack of extreme rainfall may reflect the model's limited representation of specific meteorological and climatic phenomena, such as monsoons, tropical cyclones, and localized

convective systems, which are critical drivers of extreme precipitation but may not be fully captured in long-term simulations spanning fifty to one hundred years. Furthermore, non-linear factors such as atmospheric humidity and sea surface temperature, which are essential in generating extreme rainfall and may not have been adequately incorporated. Given Malaysia's geographic location, influenced by both the Pacific and Indian Oceans, such non-linear interactions warrant explicit consideration in the modeling framework to better simulate extreme rainfall dynamics.

Moreover, the model should be periodically updated to maintain its predictive accuracy. It is also hypothesized that the absence of extreme precipitation events between 1983 and 2014 could be linked to the emergence of more extreme climatic conditions after 2014, potentially driven by factors such as urbanization, deforestation, poor land management, and agricultural expansion [16]. However, the period from 2015 to 2021 is relatively short to serve as a robust input dataset for future projections. Therefore, to achieve more accurate precipitation forecasts, it is essential to incorporate long-term datasets that include actual extreme precipitation events. One possible approach could involve integrating real observational data from 1983 to 2014 with non-linear factors observed from 2015 to 2021 such as monsoons season, El Niño and La Niña events and all influenced to varying degrees by human-induced landscape changes. This combined dataset could then be used to simulate extended historical data (1983–2021), serving as a more comprehensive foundation for future climate modeling.

Several critical considerations must be addressed to ensure the robustness and reliability of the analysis. First, the quality, completeness, and consistency of historical observational data are paramount, as all subsequent analyses rely on the integrity of this foundational dataset. Second, it is essential to verify that non-linear factors are accurately represented within the model, capturing their actual influence on precipitation dynamics. Third, rigorous validation of simulated historical data against independent observational records is necessary to evaluate both the accuracy and reliability of model outputs. Fourth, the model must be examined for consistency in temporal trends and patterns across combined datasets, ensuring that realistic changes over time are properly reflected. Additionally, special attention must be given to modeling non-linear interactions, particularly given the uncertainties inherent in the relationship between these factors and precipitation. Importantly, the assumption of stationarity may not hold, as the relationship between non-linear drivers and precipitation is likely dynamic and evolving over time. Finally, it is imperative to consider the complexities of anthropogenic influences, such as urbanization, deforestation, and land management, along with their dynamic interactions with climate variables. It must also be acknowledged that the model's ability to project future climate conditions is contingent upon assumptions made during the simulation process, which may introduce uncertainty into the projections.

Anomaly analysis was conducted by subtracting the mean historical annual rainfall observed from 2015 to 2021 at stations p1 and p2 from the projected rainfall under the SSP2-4.5 and SSP5-8.5 scenarios for the period 2022–2100. This method highlights deviations from the historical baseline, with the results illustrated in Figure 3.

Under the SSP2-4.5 scenario, a comparative assessment of rainfall anomalies between p1 and p2 reveals distinct patterns. The maximum negative anomaly at p1 is approximately –250 mm, whereas at p2, it reaches about –300 mm. Conversely, the maximum positive anomaly at p1 is estimated at 270 mm, compared to approximately 180 mm at p2. Additionally, analysing the areas enclosed by the anomaly curves (relative to the x-axis) uncovers notable differences. The area representing negative anomalies is considerably larger for p2, whereas the area corresponding to positive anomalies is more substantial for p1. These results suggest that Station 1 (p1) faces a higher risk of extreme rainfall events compared to Station 2 (p2).

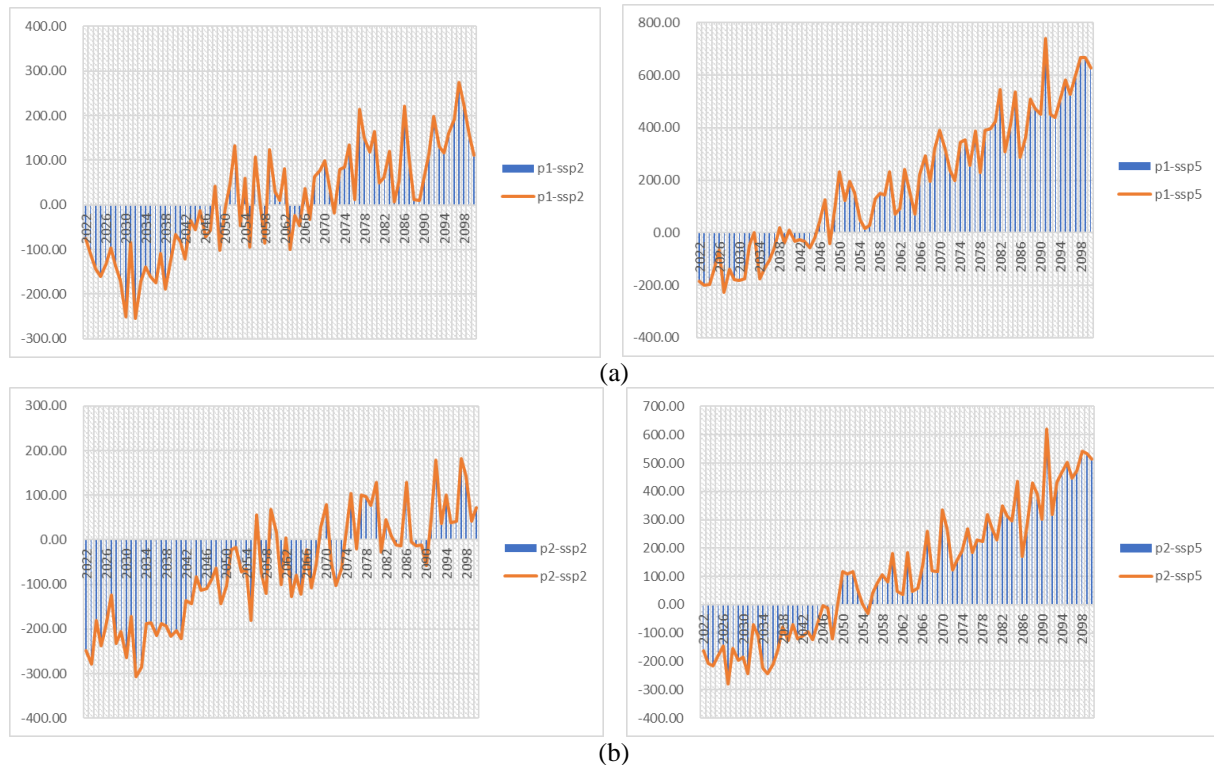
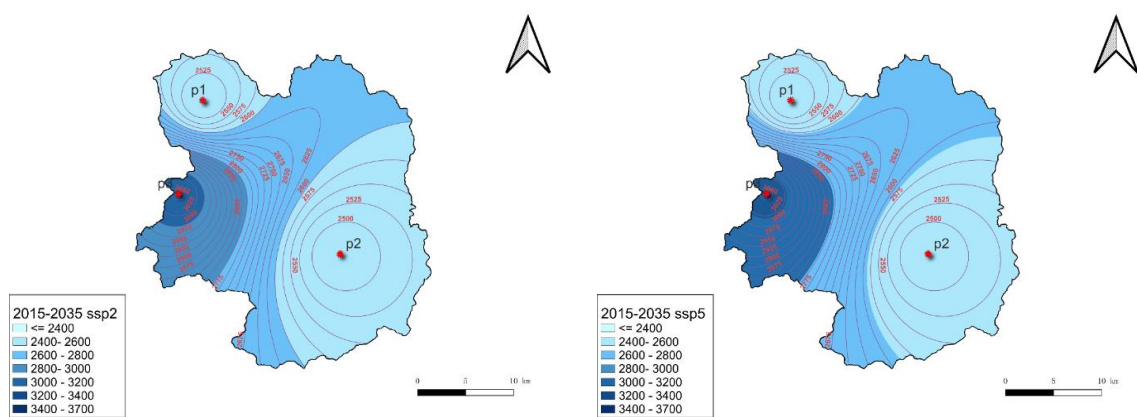


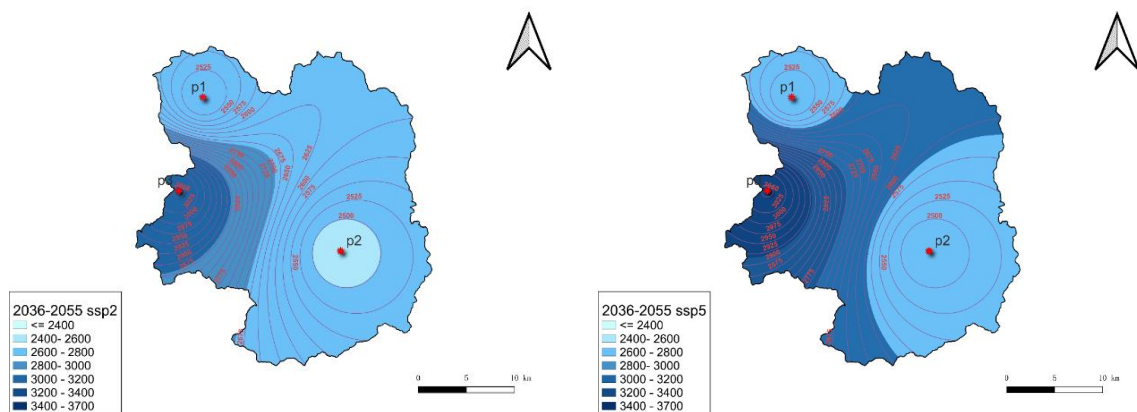
Fig. 3. Anomaly variation of Rainfall in the p1-Kg Raja and p2-Bertam Valley townships

### 3.2 Spatial analysis of future rainfall pattern

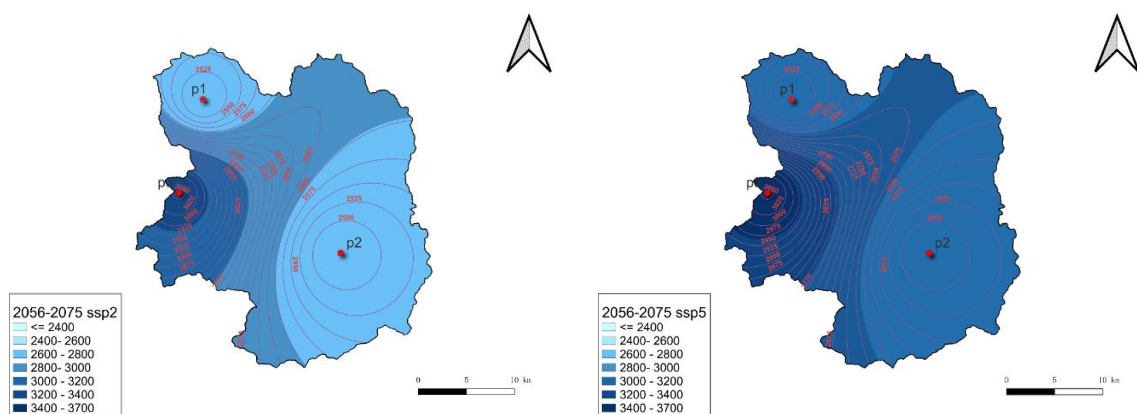
Longitudinal comparisons of rainfall variations at p1, p2, and p3 were conducted across four time-span groups (2015–2035, 2036–2055, 2056–2075, and 2076–2100) under the SSP2-4.5 and SSP5-8.5 climate scenarios. Each of time-span group representing 20 years period. Analysis of data from Table 3, in conjunction with Figure 4, reveals notable spatial and temporal patterns in rainfall distribution. For the 2015–2035 period, under SSP2-4.5, the recorded rainfall was 2499.7 mm at p1, 2479.7 mm at p2, and 3052.8 mm at p3. Under SSP5-8.5, the rainfall levels were 2495.3 mm (p1), 2503.0 mm (p2), and 3031.4 mm (p3). Notably, the p2 experienced a minor increase of 23.3 mm, while p1 and p3 saw slight decreases of 4.4 mm and 21.4 mm, respectively.



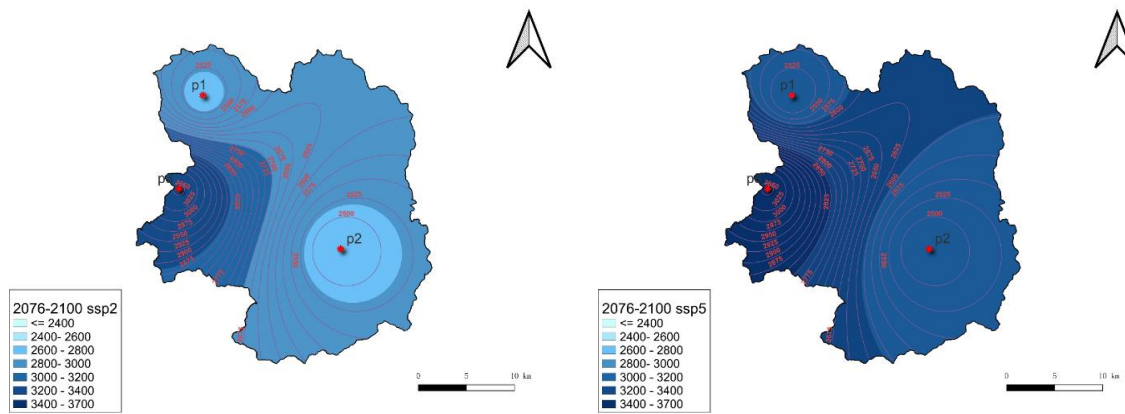
(a) 2015-2035 period



(b) 2036-2055 Period



(c) 2056- 2075 Period



(d) 2076-2100 Period

Fig. 4. Future Rainfall Pattern of Cameron Highlands based on SSP2-4.5 and 5-8.5 Scenario

Table 3. The average annual rainfall for 20-year periods

SSP2-4.5*	2015–2035	2036–2055	2056–2075	2076–2100
p1	2499.7	2602.8	2689.6	2777.9
p2	2479.7	2579.5	2675.9	2760.8
p3	3052.8	3179.2	3268.7	3379.9
SSP5-8.5*				
p1	2495.3	2688.0	2865.9	3128.6
p2	2503.1	2663.4	2850.7	3079.2
p3	3031.4	3367.2	3499.7	3606.5

For the 2036–2055 period, annual rainfall increased under both scenarios. Under SSP2-4.5, rainfall values were 2602.8 mm (p1), 2579.5 mm (p2), and 3179.2 mm (p3), whereas under SSP5-8.5, they rose to 2688.0 mm (p1), 2663.4 mm (p2), and 3367.2 mm (p3). The increases at p1, p2, and p3 were 85.1 mm, 83.8 mm, and 188.0 mm, respectively, with p3 showing a rise approximately 2.2 times higher than the average increase at p1 and p2.

For 2056–2075 period, the SSP2-4.5 projected rainfall of 2689.6 mm (p1), 2675.9 mm (p2), and 3268.7 mm (p3). Under SSP5-8.5, these amounts increased to 2865.9 mm (p1), 2850.7 mm (p2), and 3499.7 mm (p3), showing increments of 176.3 mm (p1), 174.8 mm (p2), and 231.0 mm (p3). The increase at p3 was approximately 1.3 times greater than the average increases at p1 and p2. Finally, in 2076–2100 period, the projected rainfall reached 2777.9 mm (p1), 2760.8 mm (p2), and 3379.9 mm (p3), indicating a continued upward trend in rainfall across all locations under SSP2-4.5 scenario

Regarding the temporal trends, analysis of rainfall patterns at p1, p2, and p3 across the last three time-span groups (2036–2055, 2056–2075, and 2076–2100) reveals a consistent upward trend in rainfall under both SSP2-4.5 and SSP5-8.5 scenarios. However, during the initial period (2015–2035), a slight decrease in rainfall is observed, particularly at p1 and p3 under SSP2-4.5 scenario. This decline may be attributable to specific meteorological or environmental anomalies, such as abnormal monsoon season and El Niño phenomena, which can cause temporary reductions in rainfall despite long-term increasing trends.

Analysis of rainfall patterns indicates that p3 – Brinchang consistently receives higher rainfall compared to p1 – Kg Raja and p2 – Bertam Valley. This disparity is likely attributable to the mountainous terrain of Brinchang township, where higher elevations promote rapid air cooling, favouring convection, condensation, and precipitation — a process known as orographic precipitation. Such conditions often result in persistent cloud cover and increased rainfall in elevated areas. In contrast, lowland regions, situated at lower altitudes and often shielded by surrounding mountains, are less exposed to moist air masses, thus experiencing reduced precipitation. Nevertheless, these are general patterns, and rainfall distribution may vary depending on specific geographic, climatic, and topographic factors.

Comparative analysis between scenarios indicates that, for every time-span group, rainfall under SSP5-8.5 scenario consistently exceeds that under SSP2-4.5 scenario, suggesting that higher greenhouse gas emission trajectories are associated with intensified rainfall. From a spatial perspective, Brinchang Township (p3) exhibits consistently higher rainfall than Kg Raja (p1) and Bertam Valley (p2) across all periods, reflecting the influence of topography and possibly a stronger sensitivity to climate change effects.

Given the significant rainfall increases projected for Brinchang, urgent climate adaptation and water resource management strategies are warranted. These should include enhanced flood mitigation infrastructure, efficient water resource utilization measures, and climate-resilient urban planning. Moreover, collaborative efforts among government agencies, scientists, local communities, and stakeholders are essential to develop comprehensive climate response strategies. A targeted risk assessment focusing on Brinchang's vulnerability to flooding and ecosystem shifts should be prioritized to inform effective policy and adaptation measures.

#### **4. CONCLUSION**

The analysis of the generated local climate model (2015–2100) under SSP2-4.5 and SSP5-8.5 emission scenarios reveals critical insights into future precipitation dynamics across the three study locations. Precipitation patterns for Kg Raja and Bertam Valley under both scenarios followed similar trajectories until 2063, after which they diverged notably, indicating that higher emission scenarios may induce amplified precipitation changes in the latter half of the century. In contrast, Brinchang township exhibited consistently higher precipitation than the other two locations under both scenarios, with no marked divergence observed between SSP2-4.5 and SSP5-8.5 throughout the entire period. This suggests that local geographic and climatic factors may dominate over emission-driven variability in certain regions, particularly those with complex topography and higher elevation. The spatial analysis of average annual precipitation, incorporating topographical data, highlighted the role of elevation and landform in modulating precipitation patterns. While Kg. Raja township (p1) and Bertam Valley (p2), located in lower-altitude depressions, experienced relatively moderate precipitation, Brinchang's (p3) plateau-like terrain at 1,540- 1,600 meters elevation facilitated enhanced precipitation due to orographic lifting and temperature-driven condensation processes. This relationship between altitude and precipitation emphasizes the necessity of considering topographical influences when interpreting regional climate projections. Overall, these findings suggest that future precipitation patterns are not only influenced by emission pathways but also significantly modulated by local geographic and climatic factors. Therefore, a comprehensive modeling framework is essential for capturing such complexities and for generating reliable projections to inform regional adaptation strategies.

## ACKNOWLEDGMENT

Special thanks to the MARDI, Malaysian Meteorological Department, Canadian Centre for Climate Modelling and Analysis, NASA Prediction of Worldwide Energy Resources for providing data/information.

## REFERENCES

1. IPCC 2018. Summary for Policymakers. In: Global Warming of 1.5°C. *An IPCC Special Report on the impacts of global warming of 1.5°C above pre-industrial levels and related global greenhouse gas emission pathways, in the context of strengthening the global response to the threat of climate change, sustainable development, and efforts to eradicate poverty* [Masson-Delmotte. In: Maycock, T., Tignor, M., Waterfield, T. (Eds.), Lonnoy. Press.
2. Navarre, B 2022. The 10 of the deadliest natural disasters in 2022. <https://www.usnews.com/news/best-countries/slideshows/the-deadliest-natural-disasters-in-2022> (accessed 14 March 2025).
3. Bennett, ND, Croke BFW, Guariso, G, Guillaume, JHA, Hamilton, SH, Jakeman, A, Marsili-Libelli, S, Newham, LTH, Norton, JP, Perrin, C, Pierce, SA, Robson, B, Seppelt, R, Voinov, AA, Fath, BD and Andreassian, V 2013. Characterising performance of environmental models, *Environ. Model. Software* **40**, 1–20, <https://doi.org/10.1016/j.envsoft.2012.09.011>.
4. Schoof, JT 2013. *Statistical Downscaling in Climatology*. *Geography Compass*, **7**(4), 249–265.
5. Zulkarnain, H and Sobri, H 2012. Application of Statistical Downscaling Model for Long Lead Rainfall Prediction in Kurau River Catchment of Malaysia. *Malaysian Journal of Civil Engineering* **24**(1), p1-12.
6. Chin, KS and Tan, KW 2018. Evaluation of SRE Scenarios for Penang, Selangor and Johor in Peninsular Malaysia using PRECIS Regional Climate Model (RCM). *E3S Web of Conferences*, **65**, p.05020.
7. Tahir, T, Hashim, A and Yusof, K 2018. Statistical downscaling of rainfall under transitional climate in Limbang River Basin by using SDSM. *IOP Conference Series: Earth and Environmental Science*, **140**, p.012037.
8. Noor, M and Ismail, T 2018. Downscaling of Daily Average Rainfall of Kota Bharu Kelantan, Malaysia. *Malaysian Journal of Civil Engineering* **30**(1):13-22 (2018)
9. Zaniat WNCW, Malek, MA, Md Reba, MN, Zaini, N, Ahmed, ANA, Sherif, M and El-Shafie, A 2023. Rainfall-runoff modelling based on global climate model and tropical rainfall measuring mission (GCM -TRMM): A case study in Hulu Terengganu catchment, Malaysia. *Heliyon* ,**9**(5), pp.e15740–e15740.
10. Wilby, RL and Dawson, CW 2013. The Statistical DownScaling Model: insights from one decade. *International Journal of Climatology* **33**, pp.1707–1719.
11. Department of Survey and Mapping Malaysia (JUPEM) 2002. Negeri Pahang map 1:250,000. Kuantan Malaysia
12. Wilby, RL, Dawson, CW, Murphy, C, O'Connor, P and Hawkins, E 2014. The statistical downscaling model -decision centric (SDSM-DC): conceptual basis and applications. *Clim. Res.* **61**, 251–268.
13. Siabi, EK, Kabobah, AT, Akpoti, K, Anornu, GK, Amo-Boateng, M and Nyantakyi, EK 2021. Statistical downscaling of global circulation models to assess future climate changes in the Black Volta basin of Ghana. *Environmental Challenges* **5**(100299), p.100299. doi: <https://doi.org/10.1016/j.envc.2021.100299>.

14. Wilby, RL and Dawson, CW and Barrow, EM 2002. SDSM-A decision support tool for the assessment of regional climate change impacts. *Environmental Modelling and Software* 17 (2), 145–157.
15. Tavakol-Davani, H, Nasser, M, Zahraie, B 2013. Improved statistical downscaling of daily precipitation using SDSM platform and data-mining methods. *Int. J. Climatol.* **33**, 2561–2578.
16. How Jin Aik, D, Ismail, MH, Muharam, FM, Alias, MA 2021. Evaluating the impacts of land use/land cover changes across topography against land surface temperature in Cameron Highlands. *PLoS One*,16(5):e0252111. doi: 10.1371/journal.pone.0252111.